Convolutional Coding for Direct Sequence Multicarrier CDMA*

Douglas N. Rowitch and Laurence B. Milstein

Department of Electrical and Computer Engineering
University of California, San Diego
La Jolla, CA 92093-0407 USA

ABSTRACT This paper presents a multicarrier asynchronous Direct Sequence (DS) Code Division Multiple Access (CDMA) system which, through the use of linear convolutional codes, achieves frequency diversity of an order above and beyond that realized by path diversity in a conventional RAKE DS-CDMA system. A frequency selective Rayleigh fading channel is decomposed into M frequency non-selective channels, based on the channel coherence bandwidth. Then, a rate 1/M convolutional code is used to modulate the M DS-CDMA waveforms. Diversity gains on the order of the code free distance may now be achieved. This system exhibits robust performance in the presence of narrowband interference and jamming, yet preserves the natural multiple access interference rejection properties inherent in the standard DS-CDMA model. Significant capacity gains over the single carrier system are demonstrated, while holding overall system bandwidth and information rates constant.

1 Introduction

Direct sequence CDMA has become a popular multiple access signaling methodology due in part to its robustness against fading, anti-interference capability [1,2] and multiple access capacity [3]. The large spreading bandwidths employed typically exceed the coherence bandwidth of the channel, so that the fading tends to be frequency selective. In such a situation, a RAKE receiver can be used to exploit path diversity and effectively combat the performance degradation due to multipath. In this paper, we propose an alternative to a classical RAKE receiver, in that the available bandwidth is decomposed into M equal disjoint sub-bands of bandwidth less than the coherence bandwidth of the channel. Each sub-band of the channel is assumed to fade non-selectively and independently [4,5]. In short, path diversity is exchanged for frequency diversity of an equivalent order.

This paper builds upon previous work [4,5] which examined a multicarrier DS-CDMA system that applied repetition coding and maximal ratio combining (MRC) to achieve performance similar to that of a comparable single carrier DS-CDMA system in the absence of narrowband interference. The multicarrier system was shown to exhibit superior performance in the presence of partial-band Gaussian interference. It is well known that non-trivial forward error correction coding can provide significant performance gains [6], and thus, we consider linear convolutional codes of rate 1/M, such that each user data bit produces M coded bits which, in turn, modulate M DS-CDMA waveforms that are transmitted in parallel. The receiver coherently demodulates each multicarrier signal, and the correlator outputs, appropriately weighted, drive a soft decision Viterbi decoder. Performance of this system is compared to both the single carrier DS-CDMA and the multicarrier DS-CDMA system with maximal ratio combining, in both the presence and absence of partial-band interference, while, in all cases, holding system bandwidth and information rates constant. Presented below are the system model, performance analysis and numerical results.

2 System Model

2.1 Transmitter

The transmitter for the kth user is shown in Fig. 1. The random binary data sequence $d_m^{(k)}$ is input to a rate 1/M convolutional encoder. The M code symbols, $\{x_{1,m}^{(k)}, ..., x_{M,m}^{(k)}\}$ are multiplied by the pseudo-random spreading sequence, $c_n^{(k)}$. Each user has a unique spreading sequence, and each coded symbol is held fixed over NT_c seconds (i.e., $m=\lfloor n/N \rfloor$), where T_c is the chip duration. Then, the sequence $x_{i,m}^{(k)} c_n^{(k)}$ $(i = 1,...,M)$ modulates an impulse train, where the energy per chip is E_c. After passing through a chip wave-shaping filter, each signal modulates a carrier. Thus, the transmitted signal, $s_k(t)$, is given by

$$s_k(t) = \sqrt{2E_c} \sum_{n=-\infty}^{\infty} c_n^{(k)} h\left(t - nT_c\right) \sum_{i=1}^{M} x_{i,\lfloor \frac{n}{N} \rfloor}^{(k)} \cos\left(2\pi f_i t + \theta_{k,i}\right) \quad ,(1)$$

where h(t) is the impulse response of the chip wave-shaping filter, $\theta_{k,i}$ is a random phase uniformly distributed over $[0, 2\pi)$, and M is the number of carriers.

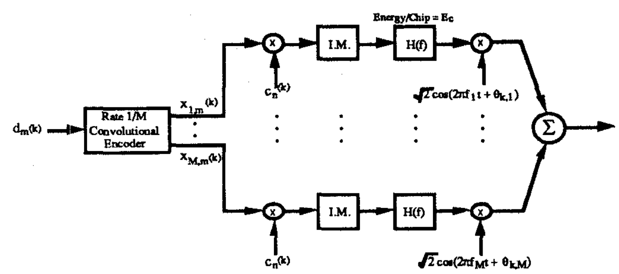

Figure 1. Transmitter for the kth User.

2.2 Channel

We assume the channel to be a slowly-varying, frequency selective, Rayleigh channel, where the DS-

* This work is supported in part by the National Science Foundation under Grant NCR-9213140.

0-7803-2489-7/95 $4.00 © 1995 IEEE

CDMA signal in each frequency band is fading non-selectively and independently [4,5]. Thus, the transfer function of the ith frequency band for the kth user is given by $\alpha_{k,i} \exp(j\beta_{k,i})$, where $\alpha_{k,i}$ and $\beta_{k,i}$ are, respectively, an i.i.d. Rayleigh random variable with a unit second moment, and an i.i.d. uniform random variable over $[0,2\pi)$ [4,5]. The received signal is given by

$$r(t)=\sum_{k=1}^{Ku}\left\{\sqrt{2E_c}\sum_{n=-\infty}^{\infty} c_n^{(k)} h\left(t - nT_c-\tau_k\right) \sum_{i=1}^{M} x^{(k)}_{i,\left\lfloor \frac{n}{N}\right\rfloor}\alpha_{k,i}\cos\left(2\pi f_i t + \theta'_{k,i}\right)\right\} + n_W(t)+n_J(t) , \quad (2)$$

where $\theta'_{k,i} = \theta_{k,i} + \beta_{k,i}$, τ_k is uniformly distributed over $[0, T_C)$ representing an arbitrary time delay, Ku is the number of multiple access users, $n_W(t)$ is additive white Gaussian noise with two-sided power spectral density $\eta_o/2$, and $n_J(t)$ is partial-band Gaussian interference with power spectral density $S_{n_J}(f)$. Fig. 2 depicts the power spectral densities of both $n_J(t)$ and the multicarrier DS-CDMA signal.

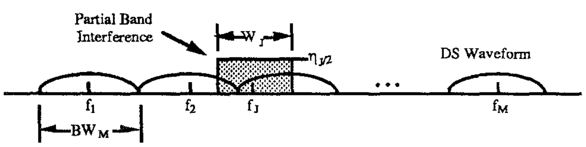

Figure 2. Channel Power Spectrum.

2.3 Receiver

The receiver of the kth user is shown in Fig. 3, where the chip wave-shaping filter is such that:

(a) $W(f) \equiv |H(f)|^2$ satisfies the Nyquist criterion,

(b) $F^{-1}\{\ W(f)\ \} \equiv w(t)$, and

(c) $\int_{-\infty}^{\infty} W(f)df \equiv 1.$ (3)

Since W(f) satisfies the Nyquist criterion, self, or inter-chip, interference may be ignored. We further assume that W(f) is bandlimited to BW_M, where $BW_M < (f_{i+1} - f_i) / 2$, and f_i is the ith carrier frequency. This implies that DS waveforms do not overlap, and therefore adjacent channel interference may be ignored.

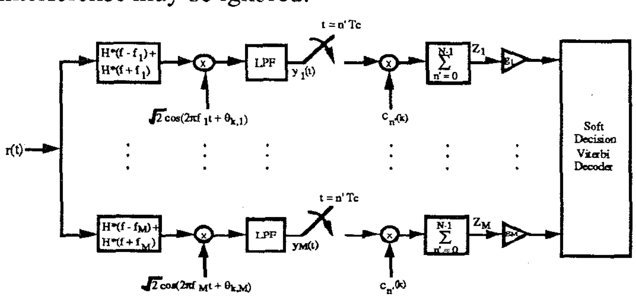

Figure 3. Receiver for the kth User.

3 Performance Analysis

3.1 Correlator Output and its Statistics

We evaluate the performance of the first user. Assuming perfect carrier, code, and bit synchronization, the output of the ith correlator branch, Z_i, is given by the sum of terms due, respectively, to the desired signal (S_{Zi}), multiple access interference (I_{Zi}), partial-band interference (J_{Zi}), and white Gaussian noise (N_{Zi}), namely

$$Z_i = S_{zi} + I_{zi} + J_{zi} + N_{zi}, \quad (4)$$

where

$$S_{zi} = \sum_{n'=0}^{N-1} c_{n'}^{(1)}\left[\sqrt{E_c}\,\alpha_{1,i}\sum_{n=-\infty}^{\infty} x^{(1)}_{i,\left\lfloor \frac{n}{N}\right\rfloor} c_n^{(1)} w(n'T_c - nT_c)\right], \quad (5)$$

$$I_{zi} = \sum_{n'=0}^{N-1} c_{n'}^{(1)}\left[\sum_{k=2}^{Ku}\left\{\sqrt{E_c}\,\xi_{k,i}\sum_{n=-\infty}^{\infty} x^{(k)}_{i,\left\lfloor \frac{n}{N}\right\rfloor} c_n^{(k)} w(n'T_c - nT_c - \tau_k)\right\}\right], \quad (6)$$

$$J_{zi} = \sum_{n'=0}^{N-1} c_{n'}^{(1)}\left[Lp\left\{n'_{J,i}(t)\sqrt{2}\cos(2\pi f_i t + \theta'_{1,i})\right\}\right], \quad (7)$$

and

$$N_{zi} = \sum_{n'=0}^{N-1} c_{n'}^{(1)}\left[Lp\left\{n'_{W,i}(t)\sqrt{2}\cos(2\pi f_i t + \theta'_{1,i})\right\}\right]. \quad (8)$$

Here, $\xi_{k,i} = \alpha_{k,i}\cos(\phi_{k,i})$ and is i.i.d. Gaussian, and $\phi_{k,i} = \theta'_{k,i} - \theta'_{1,i}$. We set $\tau_1 = 0$ without loss of generality. The terms $n'_{J,i}(t)$ and $n'_{W,i}(t)$ are, respectively, $n_J(t)$ and $n_W(t)$ after passing through the ith bandpass filter, and Lp{ } represents a lowpass filtering operation which allows us to ignore double frequency terms.

The statistics of the correlator outputs derived in [5] are presented here in summary form. We assume that the $\{c_n^{(k)}\}$ and $\{x_{i,m}^{(k)}\}$ are independent random binary sequences for k = 2, ..., Ku, while the $\{c_n^{(k)}\}$ are assumed to be deterministic for k = 1. We further make use of the fact that $w[(n' - n)T_c] = 0$ for $n' \neq n$, since W(f) satisfies the Nyquist criterion. It was shown in [5] that Z_i is conditionally asymptotically Gaussian, conditioned on $\alpha_{1,i}$ and the code symbols $\{x_{i,m}^{(1)}\}$. The conditional mean of Z_i is given by

$$S_{zi} = E\left[Z_i \,|\alpha_{1,i}, \{x_{i,m}^{(1)}\}\right] = \pm N\sqrt{E_c}\,\alpha_{1,i}, \quad (9)$$

where the algebraic sign in (9) is determined by the sign of $\{x_{i,m}^{(1)}\}$ in the appropriate bit interval. The conditional variance equals

$$\sigma_i^2 \equiv Var\left[Z_i \,|\, \alpha_{1,i}\right] = Var\left[I_{zi}\middle|\alpha_{1,i}\right] + Var\left[J_{zi}\middle|\alpha_{1,i}\right] + Var\left[N_{zi}\middle|\alpha_{1,i}\right]. \quad (10)$$

In (10), we have assumed that the interference from other users, the partial-band interference, and the additive white Gaussian noise are mutually statistically independent. In particular, we have

$$Var\left[I_{zi}\middle|\alpha_{1,i}\right] = N R_{Ii}(0) + 2\sum_{l=1}^{N-1} R_{Ii}(lT_c)\sum_{n'=l}^{N-1} c_{n'}^{(1)} c_{n'-l}^{(1)}, \quad (11)$$

$$Var\left[J_{zi}\middle|\alpha_{1,i}\right] = N R_{Ji}(0) + 2\sum_{l=1}^{N-1} R_{Ji}(lT_c)\sum_{n'=l}^{N-1} c_{n'}^{(1)} c_{n'-l}^{(1)}, \quad (12)$$

and

$$Var\left[N_{zi}\middle|\alpha_{1,i}\right] = \frac{N\eta_o}{2}. \quad (13)$$

$R_{Ii}(t)$ and $R_{Ji}(t)$ are, respectively, the autocorrelation functions of multiple access interference and partial-band interference (prior to sampling). Specifically,

$$R_{Ii}(t) = F^{-1}\{S_{Ii}(f)\} = F^{-1}\left\{\frac{(K_u - 1)E_c}{2}[W(f)]^2\right\} \quad (14)$$

and

$$R_{Ji}(t) = F^{-1}\{S_{Ji}(f)\} = F^{-1}\left\{\frac{1}{2}[S_{NJ}(f-f_i)+S_{NJ}(f+f_i)]W(f)\right\}, \qquad (15)$$

where

$$S_{NJ}(f) = \begin{cases} \frac{\eta_J}{2}, & f_J - \frac{W_J}{2} \le |f| \le f_J + \frac{W_J}{2} \\ 0, & elsewhere \end{cases} \qquad (16)$$

Since (11), (12) and (13) are independent of $\alpha_{1,i}$, the variance in (10) is unconditional.

In [5], it was assumed that the channels fade independently and hence Z_i and Z_j are uncorrelated for $i \neq j$. If, in fact, there is correlated fading between channels, then sufficient interleaving of the sequence of code symbols out of the convolutional encoder will ensure that correlator outputs are uncorrelated.

3.2 Decoder Metrics

We consider now the performance of the soft decision Viterbi decoder. Let Z_{ij} be the output of the ith correlator at time index j. Then, the branch metric for the rth path through the decoder trellis at time index j, and the path metric for the rth path are, respectively,

$$\mu_j^{(r)} = \log P\left(\overline{Z}_j \middle| \overline{X}_j^{(r)}\right) \qquad (17)$$

and

$$U^{(r)} = \sum_{j=1}^{B} \mu_j^{(r)}, \qquad (18)$$

where the vector $\overline{X}_j^{(r)}$ denotes the jth branch codeword of the rth path and B indicates either a tailed-off block size, or a decoder truncation length. If we evaluate the branch metric in terms of the joint conditional distribution of the $\{Z_{ij}\}$, and retain only terms dependent on the path index "r", we obtain

$$\mu_j^{(r)} = \sum_{i=1}^{M} \left(x_{i,j}^{(r)} z_{i,j}\right) \frac{\alpha_{i,j}}{\sigma_{i,j}^2}. \qquad (19)$$

The superscript in $x_{ij}^{(r)}$ is now taken to denote the rth path of the first user. Based on (19), we select the correlator weights, $\{g_i\}$, as channel estimates, i.e.,

$$g_{i,j} = \frac{\hat{\alpha}_{i,j}}{\hat{\sigma}_{i,j}^2}. \qquad (20)$$

For analysis, we assume perfect channel estimation.

3.3 Probability of Error

To analyze system performance, we may assume that the all-zeros path is sent, and investigate the probability of the decoder selecting some competing path [6]. The conditional probability of a path decoding error is

$$P\left(U^{(1)} \ge U^{(0)}\right) = P\left(\sum_{j=1}^{B} \sum_{i=1}^{M} z_{i,j}\left[x_{i,j}^{(1)} - x_{i,j}^{(0)}\right] \frac{\alpha_{i,j}}{\sigma_{i,j}^2} \ge 0\right), \qquad (21)$$

where r = 0 is the index of the all-zeros path and r = 1 is the index of some competing path.

Since the channel variances are not necessarily equal, due to the presence of the partial-band interference, we wish to compute the probability of a competing path containing precisely d_1 code bit errors in the first bit location (i.e., first channel), d_2 errors in the second bit location, and so on. Assuming that the variance terms do not vary over time, we define

$$P\left(d_1,\dots,d_M \middle| \alpha_1,\dots,\alpha_M\right) = P\left(\sum_{i=1}^{M} \frac{1}{\sigma_i^2} \sum_{v=1}^{d_i} z_{i,v}\alpha_{i,v} \le 0\right), \qquad (22)$$

where the index v maps to the branches containing code bit errors. The Chernoff bound on the probability in (22) is easily shown to be

$$P\left(d_1,\dots,d_M\right) \le \prod_{i=1}^{M} \left[\frac{1}{1+\overline{\gamma}_i}\right]^{d_i}, \qquad (23)$$

where $\overline{\gamma}_i \equiv \frac{N^2 E_c}{2\sigma_i^2}$ is the average signal-to-noise ratio of the correlator output of the ith channel. Note that the bound is not a function of the channel fade amplitudes, and is thus an unconditional probability. In order to use the above result to bound the average probability of bit error, we must develop a generating function for a given convolutional code which enumerates not just the number of non-zero code bits over a path, but the location (i.e., channel) of those bit errors. Then the probability of bit error may be union bounded as follows [6]:

$$P_b \le \left.\frac{dT(D_1,\dots,D_M,N)}{dN}\right|_{N=1,\ D_i=\frac{1}{1+\overline{\gamma}_i},\ i=1,\dots,M}. \qquad (24)$$

As an example, consider the rate 1/2, constraint-length 3, convolutional encoder and corresponding state diagram in Fig. 4 [7]. The state diagram below enumerates all possible paths which exit and later remerge with the all-zeros path. Branches which contain code bit errors in the first bit location are labeled with D_1, and those in the second bit location with D_2.

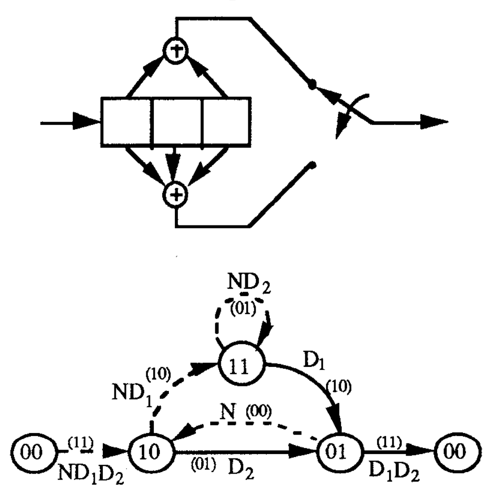

Figure 4. Convolutional Encoder and State Diagram.

The solution of the state diagram yields

$$T(D_1,D_2,N)=\frac{D_1^2D_2^3N+D_1^4D_2^2N^2-D_1^2D_2^4N^2}{1-2D_2N-D_1^2N^2+D_2^2N^2}. \quad (25)$$

Note that $T(D,D,1)=\frac{D^5}{1-2D}$, which is the result we would obtain had we ignored the code bit location. The upper bound on the probability of bit error for this code is

$$P_b \le \left.\frac{D_1^2D_2^3+2D_1^4D_2^2-D_1^4D_2^3-2D_1^2D_2^4+D_1^2D_2^5}{\left(1-2D_2-D_1^2+D_2^2\right)^2}\right|_{D_i=\frac{1}{1+\bar{\gamma}_i},\ i=1,2}. \quad (26)$$

We speculate that performance of a multicarrier system using this code will be more sensitive to partial-band interference in the second channel due to the dominant term ($D_1^2D_2^3$) of (26).

4 Numerical Results

In this section, we select for W(f) a raised-cosine spectral characteristic, where

$$W(f)=\begin{cases}\frac{1}{W_c}, & |f|\le\frac{W_c}{2}(1-\beta)\\ \frac{1}{2W_c}\left\{1-\sin\left[\frac{1}{2\beta}\left(\frac{2\pi|f|}{W_c}-\pi\right)\right]\right\}, & \frac{W_c}{2}(1-\beta)\le|f|\le\frac{W_c}{2}(1+\beta)\\ 0, & elsewhere\end{cases} \quad (27)$$

In equation (27), $W_c \equiv 1/T_c$ and β is a roll-off factor such that $0<\beta\le 1$.

In order to compare the coded multicarrier system with the single carrier RAKE DS-CDMA system, we make the following assumptions:

- overall system bandwidth and information rates are held equal,
- the transmit energy for each of the M multicarrier signals is E_b / M, where E_b is the energy per bit transmitted in the single carrier system,
- the average received energy over the M multicarrier channels is equal to the average energy received over L_1 paths in the single carrier system,
- the order of path diversity in the single carrier system is assumed identical to the number of carrier tones selected in the multicarrier system (i.e., M = L_1),
- the chip duration in the multicarrier system, T_c, is taken to be M times the chip duration of the single carrier system, T_{c1} (i.e., T_c = M T_{c1}),
- the processing gain of the multicarrier system, N, is taken to be the processing gain of the single carrier system, N_1, divided by M (i.e., N = N_1 / M),
- perfect power control; that is, the average received energy between users is assumed equal.

In the following figures, we select N_1 = 512 and M = 4, which implies that N = 128. We further select β = 0.5 as the roll-off factor for the raised-cosine filters for both multicarrier and single carrier systems.

Fig. 5 presents the probability of bit error as a function of the ratio of energy-per-bit to noise spectral density (E_b/η_o) for M = 4 and 100 multiple access users. The single carrier and multicarrier MRC systems exhibit identical performance under the above assumptions. Coded multicarrier systems using rate 1/4 convolutional codes at constraint-lengths, K = 3 and 9 are plotted with the theoretical bound from (24), as well as with simulated results. As expected, the bounds are unreliable at low bit error rates (BER) due to the union bound in (24). We see a significant coding gain for increasing code constraint-length.

Fig. 6 plots BER versus the number of multiple access users, Ku, for M=4 and E_b/η_o = 7 (dB). It is seen that significant user capacity can be realized for sufficiently large E_b/η_o and/or constraint-lengths.

In Fig. 7, we introduce partial-band interference (PBI), and depict BER versus the jamming-to-signal power ratio (JSR) for M=4, Ku = 100, and E_b/η_o = 10 (dB). Here, the PBI is centered on the second multicarrier channel with bandwidth equal to that of the second channel. As shown, the multicarrier systems are less sensitive to PBI, and can provide desired BER performance at moderate to high JSR levels for sufficiently large code constraint-lengths.

In Fig. 8, we vary the center frequency of the (PBI) and plot average probability of bit error for M=4, Ku = 100, E_b/η_o = 10 (dB), and JSR = 30 (dB). Here, the PBI bandwidth is equal to that of one multicarrier channel. The coded multicarrier systems exhibit superior performance when the PBI effects only one channel; when the PBI overlaps two adjacent channels, significant performance degradation is seen. This is due to the sensitivity of code performance to burst errors and can be mitigated by sufficient interleaving of the coded symbols. Note also that the K=3 code is particularly sensitive to PBI in the first channel, as is the K=7 code to PBI in the fourth channel, whereas the K=9 code is relatively insensitive with respect to which channel experiences the PBI. This behavior is explained by the distribution of code bit errors for the minimum distance path error events. For the rate 1/4, K=3 code, the dominant term in the generating function is $D_1^4D_2^2D_3^2D_4^2$, from which it is clear that performance will suffer more when PBI resides in the first channel since it makes the minimum distance error event more likely. Performance of the single carrier system is significantly degraded regardless of the location of the interference.

Finally, Fig. 9 displays BER versus E_b/η_o for JSR values of 0 (dB) and 30 (dB). Here, M=4, Ku = 100 and we use a rate 1/4, K=7 code. For this code, at a BER of 10^{3}, we can effectively compensate for a JSR of 30 (dB) by an increase of approximately 2 (dB) in E_b/η_o.

5 Conclusions

In this paper, we have presented a viable alternative to the conventional RAKE DS-CDMA system. As demonstrated, the multicarrier system effectively suppresses narrowband interference and exhibits robust behavior in the presence of Rayleigh fading, while still maintaining the desirable multiple access interference rejection properties inherent in DS-CDMA systems. Under the assumption of equal total bandwidth and information rates, the multicarrier system more efficiently utilizes the available time/frequency space, by trading path diversity for frequency diversity, wherein forward error correction coding may be employed to achieve noticeable gain in user capacity.

REFERENCES

[1] G. L. Turin, "Introduction to Sprea d-Spectrum Antimultipath Techniques and Their Application to Urban Digital Radio," *Proc. IEEE.*, vol. 68, No. 3, pp. 328-353, March 1980.

[2] R. L. Pickholtz, D. L. Schilling, and L. B. Milstein, "Theory of Spread-Spectrum -- A Tutorial," *IEEE Trans. Commun.*, vol. COM-30, No. 5, pp. 855-884, May 1982.

[3] Viterbi, A. J., "Wireless Digital Communication: A View Based on Three Lessons Learned," *IEEE Commun. Mag.*, pp. 33-36, September 1991.

[4] S. Kondo and L. B. Milstein, "Multicarrier DS CDMA Systems in the Presence of Partial Band Interference," *Proc. MILCOM'94*, Fort Monmouth, NJ, October 1994.

[5] S. Kondo and L. B. Milstein, "On the Performance of Multicarrier DS CDMA Systems," submitted to *IEEE Trans. Commun.*

[6] J. Proakis, *Digital Communications*. New York: McGraw-Hill, 1989.

[7] K. J. Larsen, "Short Convolutional Codes with Maximal Free Distance for rates 1/2, 1/3, and 1/4," *IEEE Trans. Inform. Theory*, vol. IT-19, pp. 371-372, May 1973.

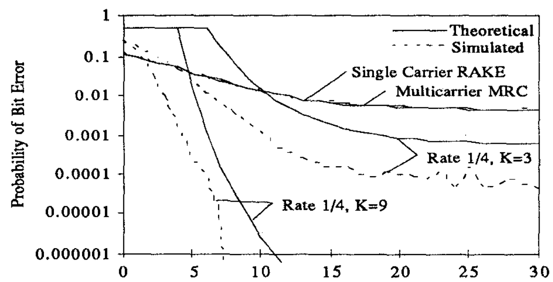

Figure 5. BER vs. E_b/η_0.

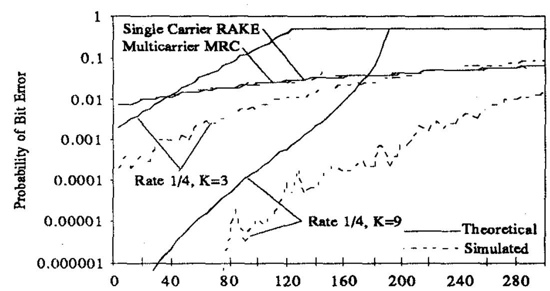

Figure 6. BER vs. Ku.

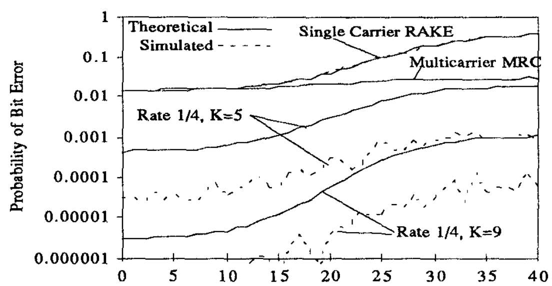

Figure 7. BER vs. JSR.

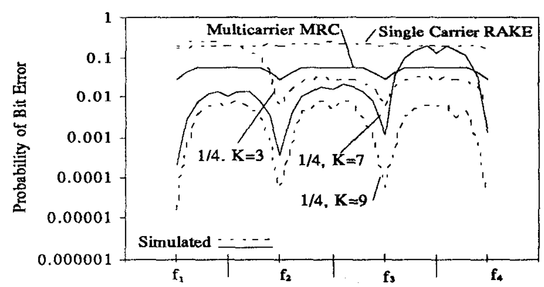

Figure 8. BER vs. f_J.

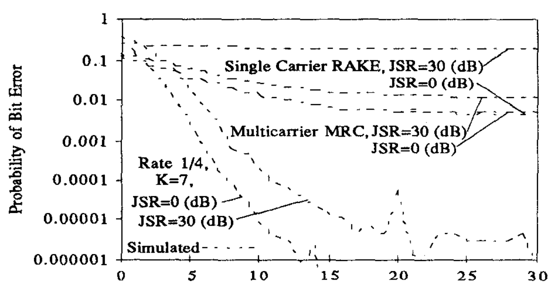

Figure 9. BER vs. E_b/η_0.